Expression of a functional Kir4 family inward rectifier K^+ channel from a gene cloned from mouse liver

Wade L. Pearson *, Michelle Dourado †, Matthew Schreiber †, Lawrence Salkoff † and Colin G. Nichols *

*Department of Cell Biology and Physiology and †Department of Anatomy and Neurobiology, Washington University School of Medicine, St Louis, MO 63110, USA

(Received 4 June 1998; accepted after revision 13 October 1998)

1. A low stringency polymerase chain reaction (PCR) homology screening procedure was used to probe a mouse liver cDNA library to identify novel inward rectifier K^+ channel genes. A single gene (mLV1) was identified that exhibited extensive sequence homology with previously cloned inward rectifier K^+ channel genes. The mLV1 gene showed greatest sequence identity with genes belonging to the Kir4 subfamily. The amino acid sequence of mLV1 was 96% identical to a Kir channel cloned from human kidney (hKir4.2), and ~60% identical to the Kir4.1 channel cloned from human and rat, so that mLV1 was classified as mKir4.2.

2. *Xenopus* oocytes injected with cRNA encoding mKir4.2 displayed a large inwardly rectifying K^+ current, while control oocytes injected with H_2O displayed no similar K^+ current. The current was blocked by Ba^{2+} and Cs^+ in a voltage-dependent fashion and displayed inward rectification that was intermediate between that of the strong inward rectifier Kir2.1 and the weak inward rectifier Kir1.1. The current was weakly blocked by TEA in a voltage-independent fashion.

3. mKir4.2 current was subject to modulation by several distinct mechanisms. Intracellular acidification decreased mKir4.2 current in a reversible fashion, while activation of protein kinase C decreased mKir4.2 current in a manner that was not rapidly reversible. Incubation of oocytes in elevated $[K^+]$ produced a slowly developing enhancement of current.

4. Oocytes co-injected with cRNA for mKir4.2 and Kir5.1, a protein that does not form functional homomeric channels, displayed membrane currents with properties distinct from those expressing mKir4.2 alone. Co-injected oocytes displayed larger currents than mKir4.2, with novel kinetic properties and an increased sensitivity to Ba^{2+} block at negative potentials, suggesting that mKir4.2 forms functional heteromultimeric channels with Kir5.1, as has been shown for Kir4.1

5. These results demonstrate for the first time that a Kir4.2 channel gene product forms functional channels in *Xenopus* oocytes, that these Kir channels display novel properties, and that Kir4.2 subunits may be responsible for physiological modulation of functional Kir channels.

Since the cloning of the first inward rectifier K^+ channel, ROMK1 (Kir1.1a: Ho *et al.* 1993), a large family of related Kir channel genes has been identified. These genes have been divided into seven subfamilies (to date) based on their predicted protein sequences (Doupnik *et al.* 1995), and there is a strong correlation between structure and function within each subfamily. Kir3 channel activity is modulated by G-protein $\beta\gamma$ subunits (Reuveny *et al.* 1994), Kir6 channel activity is modulated by intracellular [ATP] (Inagaki *et al.* 1995), Kir2 channels are strong inward rectifiers, and are subject to modulation by various effectors including extracellular pH (Coulter *et al.* 1995), intracellular [ATP] (Collins *et al.* 1996), PKC activity (Henry *et al.* 1996), G-protein (Cohen *et al.* 1996), and $[Mg^{2+}]$ (Chuang *et al.* 1997), and Kir1 and Kir4 channel activity is subject to modulation by intracellular pH (Tsai *et al.* 1995; Doi *et al.* 1996; Fakler *et al.* 1996; Shuck *et al.* 1997). An additional level of complexity of channel function arises from the demonstration that some Kir channels form as heteromultimers in native tissue (Kir3 channels, Krapivinsky *et al.* 1995), or require additional protein subunits to form functional channels (Kir6 channels: Inagaki *et al.* 1995). However, relatively little is known about

the molecular correlates of channels in native tissue and whether the channels form as homo- or heteromultimers. Kir4.1 channel subunits have been demonstrated to form heteromultimeric channels with Kir1.1 (Glowatzki *et al.* 1995) and Kir5.1 (Pessia *et al.* 1996). Because the function of a heteromultimeric channel can be affected by the activity of a single subunit, it is important to know how the activity of each subunit can be modulated in homomeric expression.

The first Kir4 channel, Kir4.1 (variously named BIR10, KAB-2 or BIRK1) was cloned from rat brain (Bond *et al.* 1994; Bredt *et al.* 1995; Takumi *et al.* 1995). In the last year, other members of this subfamily have been cloned from salmon brain (Kubo *et al.* 1996) and from human kidney and skeletal muscle (Gosset *et al.* 1997; Ohira *et al.* 1997; Shuck *et al.* 1997). While some confusion over channel nomenclature persists (see Discussion), the channel best classified as Kir4.2 cloned from human kidney has been reported not to express functional channels in *Xenopus* oocytes (Shuck *et al.* 1997). In this paper, we report the successful expression of a Kir4.2 channel cloned from mouse liver. The expressed channel is an inward rectifier, but is subject to a unique combination of modulatory mechanisms, including sensitivity to changes in intracellular pH, protein kinase C (PKC) activity, and extracellular $[K^+]$ ($[K^+]_o$).

METHODS

Molecular biology

Low stringency polymerase chain reaction (PCR) homology screening of a mouse liver cDNA library was performed to identify novel Kir channel clones. Two successive PCRs were performed using degenerate primers in the first round followed by complementary non-degenerate primers in the second round for reamplification of the products for subcloning. Specifically, degenerate primers corresponding to the coding sequence Thr-Ile-Gly-Tyr-Gly (pore) and Pro-Lys-Lys-Arg (C-terminal to the M2 domain) were employed in the first round of PCR (36 cycles) with a mouse liver cDNA library as template. Products of approximately 189 base pair (bp) size were isolated on low melting temperature agarose gels. The products were then used as templates in a second reamplification PCR (30 cycles) with corresponding non-degenerate primers. The sequences of the degenerate first round (D) and non-degenerate second round (N) PCR oligonucleotides are given in Table 1. The products of the second round were cut with restriction enzymes *Eco*RI and *Xba*I (engineered into the oligonucleotides) and subcloned into M13 mp18 vector for sequencing. The mLV1 (mouse liver 1) PCR fragment was identified by high homology to inward rectifier K^+ channel pore and downstream membrane-spanning domain sequences. The PCR fragment was used to generate a probe for high stringency screening of the mouse liver cDNA library. The probe was generated using a random hexamer primed extension reaction (Ambion, Austin, TX) with [^{32}P]-labelled deoxycytidine 5′-triphosphate. The mouse liver cDNA library in λ-ZAP was plated at high density on large culture plates (~10^5 colonies per plate). The plaques were blotted onto nitrocellulose, fixed, and dried. The probe hybridization was carried out using standard high stringency conditions in buffer containing 0·1% SDS at 60 °C. λ-ZAP clones hybridizing to the probe were plaque purified and inserts were excised following the standard ZAP protocol into the pBluescript II SK^+ plasmid for sequencing. Two identical clones were isolated which included the entire deduced mLV1 open reading frame. The entire open reading frame was sequenced in both directions and was closed upstream of the putative initiator methionine. The expression vector was generated by PCR with an oligonucleotide including the Kozak (Kozak, 1987) initiation sequence at the initiator methionine. The PCR product was then subcloned into the expression vector pBScMXT (Wei *et al.* 1994) for expression in *Xenopus* oocytes. The entire expression vector was sequenced to ensure the absence of PCR introduced errors. For cRNA transcription, the template was purified by CsCl gradient centrifugation and RNA was transcribed *in vitro* using Message Machine transcription kits (Ambion).

Expression in oocytes

Oocytes were isolated from *Xenopus laevis* by partial ovariectomy under tricaine anaesthesia, and defolliculated as described previously (Henry *et al.* 1996). After defolliculation, oocytes were stored in ND96 solution (see below) supplemented with penicillin (100 units ml^{-1}), streptomycin (100 μg ml^{-1}) and 1·8 mM $CaCl_2$. Oocytes were pressure injected with ~50 nl RNA (1–100 ng μl^{-1}) through bevelled micropipettes. RNA was diluted to a suitable concentration with distilled H_2O treated with diethylpyrocarbonate to minimize RNA degradation. For co-expression experiments, mKir4.2 cRNA was first diluted to an appropriate working concentration, and then mixed with an equal volume of H_2O or Kir5.1 cRNA to keep the total amount mKir4.2 cRNA constant.

Electrophysiology and data analysis

Two-electrode voltage-clamp experiments were performed on oocytes placed in a Plexiglass chamber constantly perfused by gravity flow through multiple inlet lines allowing rapid solution changes. Recording electrodes were pulled from thin-walled borosilicate glass (TW-150-F4, WPI, Sarasota, FL, USA), filled with 3 M KCl, and had initial resistance of 0·3–1·0 MΩ. The recording chamber was connected to the electronics via Ag–AgCl electrodes in 1% agar bridges. Chamber volume was ~600 μl, and ~95% solution exchange occurred in less than 1 min. All experiments were performed at room temperature (~23 °C). Currents were recorded with an OC-725 Oocyte Clamp (Warner Inst. Co, Hamden, CT, USA) controlled by pCLAMP software (Axon Instruments, Foster City, CA, USA). Data were typically digitized at 0·5–1·0 kHz and recorded directly to disk. Data analysis was performed with Igor Pro software (Wavemetrics, Lake Oswego, OR, USA). For accurately quantifying the effect of channel blockers on mLV1 channel activity, it was occasionally necessary to estimate the amplitude of current activated by prolonged high $[K^+]$ exposure during channel blocker application. Control experiments (not shown) indicated that for $[K^+]$ exposures ~20 min in duration, current increased approximately linearly with time, so that the control (i.e. unblocked) current amplitude for any measurement could be estimated (I_{est}) by adding a proportion of K^+-activated current ($I_{est} = I_O + (t_{int}/t_{F-O})(I_F - I_O)$, where t_{int} is the duration between the original control measure (I_O) and the test measurement, I_F is the final control measure, and t_{F-O} is the duration between the original and final control measures).

Solutions and chemicals

Two electrode voltage-clamp experiments were performed in solutions based on the following compositions. ND96 (mM): 2 KCl, 96 NaCl, 1 $MgCl_2$, 5 Na-Hepes; NMG96 (mM): 2 KCl, 96 *N*-methyl-D-glucamine (NMG)-Cl, 1 $MgCl_2$, 5 NMG-Hepes; KD98 (mM): 98 KCl, 1 $MgCl_2$, 5 K-Hepes (i.e. ~100 mM K^+).

The pH of all solutions was adjusted to 7·5. For solutions of intermediate $[K^+]$ used in measuring relative conductance (G_{rel}) and reversal potential (V_{rev}), $[K^+]$ was adjusted by substituting KCl for

Table 1. Sequences of the degenerate first round (D) and non-degenerate second round (N) PCR oligonucleotides

Pore (sense) primers	
D	T TCTCCT TCTAGACTCA A ACTAC(N)AT(T/C/A)GG(N)(C/T)GG
N	T TCTCCT TCTAGACTCA A ACTAC
M2 (antisense) primers	
D	ATGAGA AT TCTAGTGT T TCTGCTC(T/G)(T/C)T T(T/C)T T(N)GG
N	ATGAGA AT TCTAGTGT T TCTGCTC

Degenerate positions are given in parentheses and N indicates A, C, G, or T at a given position.

NMG-Cl in the NMG96 solution. For experiments testing channel block, TEA-Cl, $BaCl_2$ and CsCl (Sigma) were added directly to the KD98 solution without adjusting osmolarity. To study the effects of intracellular acidification, ND96 and KD98 solutions were altered by substituting 50 mM $NaHCO_3$ or $KHCO_3$ for 50 mM of the appropriate Cl^- salt. Solutions containing HCO_3^- were prepared fresh before the experiment each day. For studying the effects of protein kinase C activation, stock solutions (10 mM) of the phorbol esters phorbol 12-myristate 13-acetate (PMA), phorbol 12,13-dibutyrate (PDBU), and 4α-phorbol 12,13 didecanoate (4α-PDD) (Sigma) were dissolved in dimethylsulfoxide (DMSO) and diluted to working concentration directly before use. Application of equal concentrations of DMSO without phorbol esters was without effect on mKir4.2 channels.

Nomenclature

In this paper we attempt to refer to cloned inward rectifier channels by a standard nomenclature devised by Doupnik *et al.* (1995). Thus, the ROMK1 (Ho *et al.* 1993) channel will be referred to as Kir1.1, and IRK1 (Kubo *et al.* 1993) will be referred to as Kir2.1. References for the identification of other channels not explicitly discussed in the text can be found in a recent review (Nichols & Lopatin, 1997).

RESULTS

Cloning of a novel Kir channel from mouse liver

mLV1 was cloned from a mouse liver cDNA library using the PCR technique with degenerate primers based on conserved sequence motifs (see Methods). A novel PCR product encoding a portion of the K^+ channel pore and M2 domain was isolated, labelled, and used as a high stringency probe for screening the cDNA library. Two positive clones were obtained from the 10^6 clones screened. Sequencing showed that the two clones were identical. The clone contained an open reading frame encoding a protein of 375 amino acid residues, which was homologous to other cloned inward rectifiers (Fig. 1*A*; entire nucleotide sequence deposited in GenBank, Accession No. AF085696). A channel recently cloned from human kidney and skeletal muscle (hKir4.2: Gosset *et al.* 1997; Ohira *et al.* 1997; Shuck *et al.* 1997) was 96% identical at the amino acid level. Thus, mLV1 was classified as mKir4.2 (see Discussion). The protein sequence was compared with the other members of the Kir channel family by using a Clustal sequence alignment. The resulting phylogenetic tree showed that this gene product was most closely related to the Kir4.1 channel (i.e. BIR10: Bond *et al.* 1994; KAB-2: Takumi *et al.* 1995). The relative distance between mKir4.2 and other Kir4 channels was similar to distances between channels within other Kir channel subfamilies, while the distance between mKir4.2 and Kir1.1 was greater than that between members of other previously defined Kir subfamilies (Fig. 1*B*). Comparing the mKir4.2 sequence against the Prosite database (Appel *et al.* 1994) revealed the presence of four strong consensus sequences for phosphorylation by protein kinase C (Ser/Thr-X-Arg/Lys) and two for tyrosine phosphorylation (Arg/Lys-X-X-(X)-Asp/Glu-X-X-(X)-Tyr) (Fig. 1*A*). Two potential sites for N-linked glycosylation (Asn-X-Ser/Thr) were also found, although the Asn284 site is unlikely to be of significance because it is located on a presumed cytoplasmic region. A previously identified glycosylation site in Kir1.1 also exists in mKir4.2 (Asn103). However, the ATP-binding motif found in Kir1.1 is not present in mKir4.2 (Ho *et al.* 1993).

Heterologous expression in *Xenopus* oocytes

To determine whether the clone expressed functional ion channels, we injected *Xenopus* oocytes with *in vitro* transcribed mKir4.2 cRNA. After 18–48 h, cells injected with mKir4.2 RNA had very negative ($-84{\cdot}2 \pm 6{\cdot}4$ mV, $n = 5$) resting potentials in 2 mM K^+, 96 mM Na^+ solution, while water-injected oocytes had more depolarized resting potentials ($-35{\cdot}0 \pm 2{\cdot}3$ mV, $n = 5$). Using the two-electrode voltage clamp technique, large K^+ currents were measured in oocytes injected with mKir4.2 RNA (Fig. 2*A*). The mKir4.2 current was inward at potentials negative to the K^+ reversal potential (E_K). At potentials positive to E_K, currents were outward, and rectified inwardly at depolarized potentials. Whole-cell reversal potential shifted to more positive values with increasing K^+ concentration (46 mV per tenfold increase in extracellular $[K^+]$ ($[K^+]_o$), $n = 11$) (Fig. 2*B* and *C*), indicating that the channel is largely K^+ selective. The discrepancy between the 46 mV per decade shift and that predicted for a perfectly selective channel (58 mV per decade) may be attributed to additional membrane conductance from other (probably Cl^-) channels expressed in the oocytes (see Fig. 2*A*). In addition to changes in reversal potential, the conductance increased with increasing $[K^+]_o$. In native and other cloned inward rectifier channels, conductance (G) increases in proportion to $[K^+]_o^{0.5}$ (Hagiwara & Takahashi, 1974; Ho *et al.* 1993;

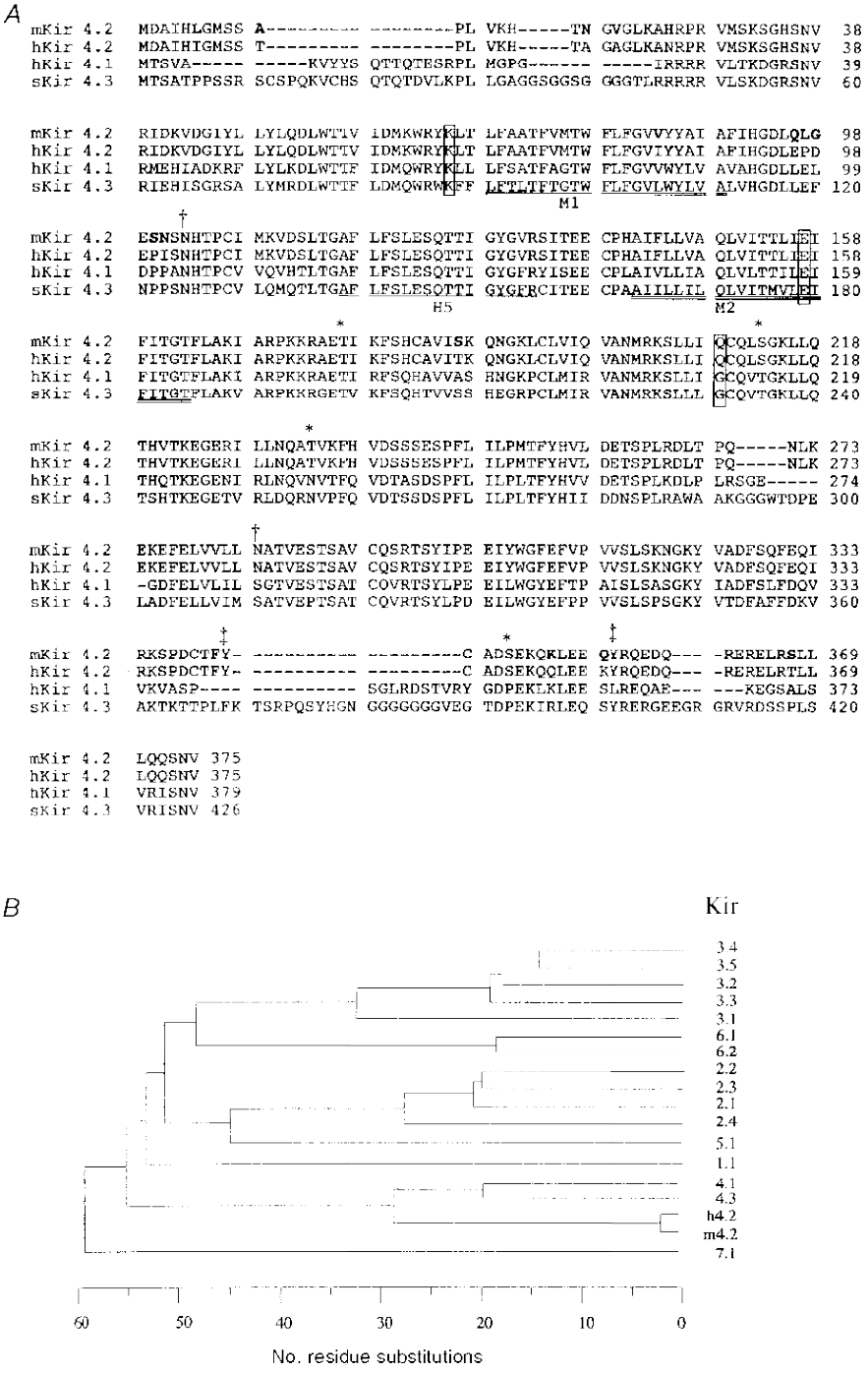

Figure 1. The mLV1 (mKir4.2) gene encodes a Kir channel protein

A, alignment of the amino acid sequences of representatives Kir4 family members. Bold-face letters in the mKir4.2 sequence indicate residues differing from hKir4.2. Double underlining indicates the proposed transmembrane domains (M1 and M2) while single underlining indicates the pore region (H5). Consensus sites for PKC phosphorylation (*), tyrosine kinase (†), and glycosylation (‡) are indicated. Boxes around Glu157 and Gln209 indicate the presence and absence, respectively, of charged residues at the 'rectification controller' positions. Lys66 is boxed to show its presence at the site implicated in sensitivity to intracellular pH. Alignments were performed with Megalign software (DNASTAR, Inc., Madison, WI, USA) using the Clustal method. *B*, dendrogram of the Kir channel family. Relationships are shown as a balanced branched cladogram. The scale indicates residue substitutions from a hypothetical ancestral protein. Genes cloned from mouse were used in the alignment where possible. Genbank accession numbers for Kir channel sequences used are as follows: mouse 2.1 (X33052), 2.2 (X00417), 2.3 (U11075), 3.1 (D45022), 3.2 (U11859), 3.3 (U11860), 3.4 (U33631), 4.2 (AF085696) 6.1 (D88159), 6.2 (U73626); rat 1.1 (X22341), 2.4 (AJ003065), 4.1 (X33585), 5.1 (X33581), 7.1 (AJ006129); human 4.2 (U73191); *Xenopus* 3.5 (U42207); salmon 4.3 (D83537).

Kubo *et al.* 1993). To determine the relationship between $[K^+]_o$ and G, we estimated the current amplitude (i.e. relative conductance, G_{rel}) by interpolation at a membrane potential 40 mV negative to the reversal potential (V_{rev}) for four different $[K^+]_o$ and fitted the equation $G_{rel} = k[K^+]_o{}^n$ to the data, with the scaling factor k and the exponent n left as free coefficients (Fig. 2*D*). For data averaged from 7 cells, $n = 0{\cdot}66$, which is in general agreement with the previous reports ($n \approx 0{\cdot}5$). A slow increase in current amplitude on exposure to elevated $[K^+]$ may account for the exponent exceeding previous measurements (see below).

By definition, an inward rectifier channel has a greater conductance for inward current than for outward current, and inward rectification is typically either strong or weak as a result of different sensitivities to intracellular polyamines and Mg^{2+} (Nichols & Lopatin, 1997). We compared inward rectification of mKir4.2 channels with the inward rectification of a strong inward rectifier (Kir2.1) and weak inward rectifier (Kir1.1) (Fig. 2*E*). mKir4.2 showed a distinct reduction in the slope conductance of outward current compared with inward current in low $[K^+]_o$ solutions, although the effect was more obvious in high

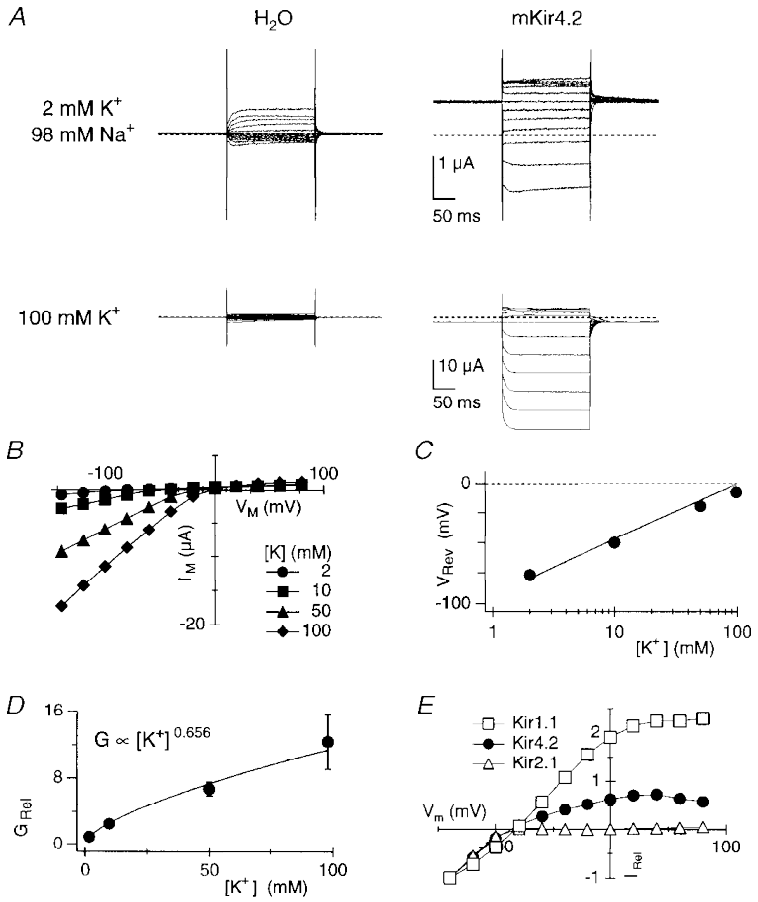

Figure 2. Properties of Kir4.2 currents expressed in *Xenopus* oocytes

A, currents recorded from *Xenopus* oocytes injected with H_2O or cRNA encoding mKir4.2. H_2O-injected oocytes displayed little inward current and a small time- and voltage-dependent outward current at depolarized potentials (probably a Ca^{2+}-activated Cl^- current). In contrast, mKir4.2-injected oocytes displayed a large inwardly rectifying current. Cells were held at −20 mV and stepped to potentials between −140 and 80 mV in 20 mV increments for 200 ms every 0·5 s. *B*, representative whole-cell current (I_m)–voltage (V_m) relations recorded from an oocyte injected with mKir4.2 cRNA in solutions of increasing $[K^+]$. Recordings were made ~2–3 min after solution changes began to ensure exchange was complete. Measurements were made at the end of 200 ms test pulses. Leak current was relatively small and thus was not subtracted from these records. *C*, whole-cell reversal potential (V_{rev}) shifts with $[K^+]_o$. Straight line shows least-squares fit of V_{rev} *vs.* $\log[K^+]_o$, assuming intracellular $[K^+]$ to be 100 mM. V_{rev} changed 46·7 mV per tenfold change in $[K^+]_o$. *D*, conductance was estimated by interpolating current amplitude at a potential 40 mV below the apparent reversal potential. Data were collected from the same experiments used for measuring reversal potential. Continuous line indicates fit to the function $G_{rel} = k[K^+]^n$, where the exponent n and scaling factor k were left as free coefficients. *E*, steady-state current–voltage relationships measured in 2 mM K^+ (ND96) for mKir4.2, rKir2.1, and rKir1.1 channels. Currents (I_{rel}) were normalized at −140 mV to compare the voltage dependence of the different channels.

$[K^+]_o$ solutions (Fig. 2*B*). In low $[K^+]_o$ solutions, a region of negative slope conductance is apparent at potentials over +40 mV. We also examined the ability of Ba^{2+} and Cs^+, common Kir channel blockers, to block mKir4.2. mKir4.2 channels were blocked by Ba^{2+} and Cs^+ in a steeply voltage-dependent fashion (Fig. 3). In contrast, TEA blocked mKir4.2 current poorly (K_i ~10 mM at −60 mV) (Fig. 3), although more effectively than it blocked Kir2.1 current (10 mM TEA reduced Kir2.1 current ~20%, data not shown).

Novel properties of the mLV1 current

Slow current enhancement on continued exposure to high $[K^+]_o$ solution. Upon exposure to high extracellular $[K^+]$ ($[K^+]_o$), the amplitude of mKir4.2 current increased in a biphasic manner. A rapid component of current increase occurred within 1 min of solution change, attributable primarily to the changes in driving force and the $[K^+]$ dependence of conductance, followed by a slower component which we will refer to as 'K^+ activation' (Fig. 4*A*). In contrast to mKir4.2, oocytes from the same batch expressing Kir2.1 channels showed only a rapid increase in current amplitude on changing to high $[K^+]_o$ (Fig. 4*A*), indicating that K^+ activation cannot be a general property of all Kir channels. For high $[K^+]_o$ exposures of ~20 min, increases in current amplitude as large as fourfold were measured (Fig. 4*B*). However, preliminary experiments indicated that additional K^+ activation continued for periods at least as long as 1 h (data not shown). Long-term preincubation of oocytes in high $[K^+]_o$ solution increased the initial current in low $[K^+]_o$ solutions, and slowed subsequent K^+ activation, indicating that K^+ activation is a saturable process (Fig. 4*C*). Slow changes in the ionic composition of the bathing solution could not account for such prolonged increases in current (< 1 min for ~95% exchange of bath solution). Because the K^+ activation process occurs so slowly, it seems likely to

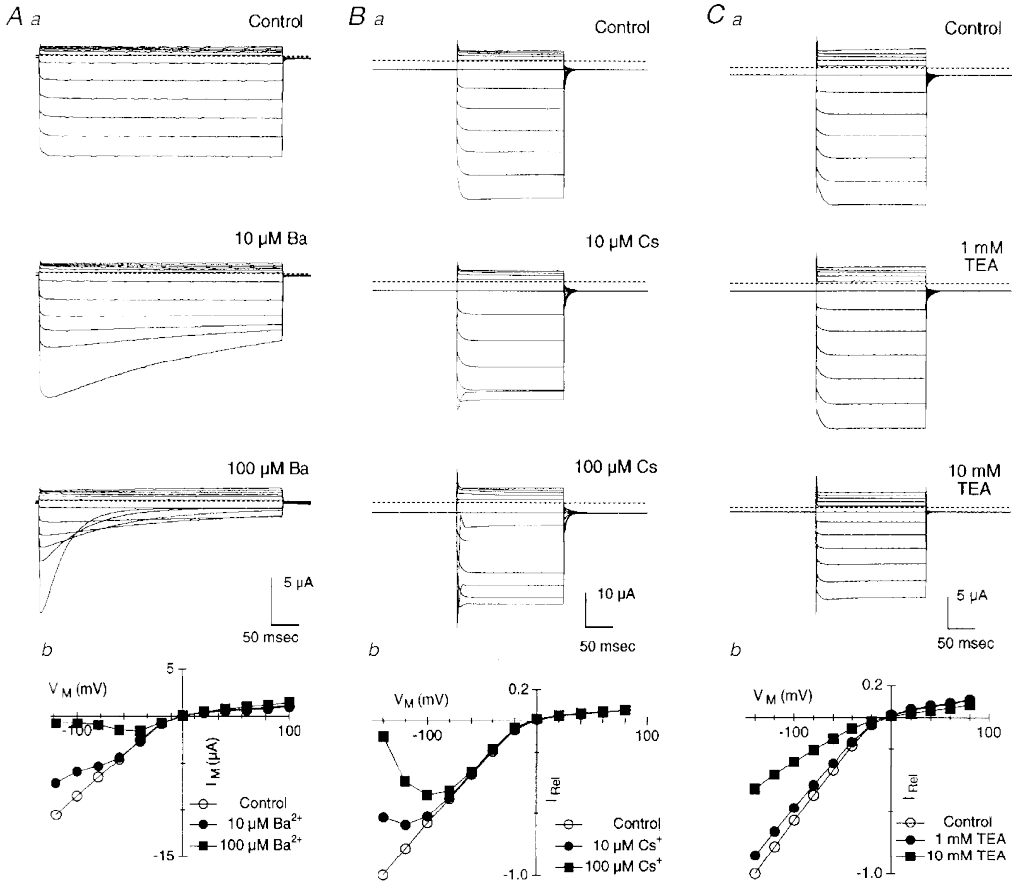

Figure 3. mKir4.2 currents are sensitive to external Ba^{2+}, Cs^+ and TEA

Aa, current traces show block of mKir4.2 current by 10 and 100 μM Ba^{2+}. Note that channel block by Ba^{2+} is not instantaneous, and that the rate of channel block increases at more negative potentials. *Ab*, *I–V* curves show voltage dependence of channel block. *Ba*, Cs^+ blocks mLV1 channels in a voltage-dependent fashion. Channel block occurs more rapidly than with Ba^{2+}. *Bb*, *I–V* curves show Cs^+ block to be more voltage dependent than Ba^{2+} block. *Ca*, TEA blocks mLV1 channels poorly. Current traces show that block develops instantaneously (however, little time-dependent change is expected because the voltage dependence is low). *Cb*, *I–V* curves show that high concentrations of TEA (10 mM) partially block mKir4.2 current at negative membrane potentials. Control *I–V* curves have been adjusted to account for on-going K^+ activation (see Methods).

result from a cellular process evoked by changing $[K^+]_o$, rather than from a direct effect of $[K^+]_o$ on the channel. On returning to low $[K^+]_o$ solutions, K^+ activation reversed slowly (Fig. 4*D*). No enhancement of mKir4.2 current amplitude was seen on changing the bath to low $[K^+]_o$ solutions in which Na^+ had been replaced by NMG^+, indicating that the increase in current resulted from increases in $[K^+]_o$, not decreases in $[Na^+]_o$ (Fig. 4*A*). This

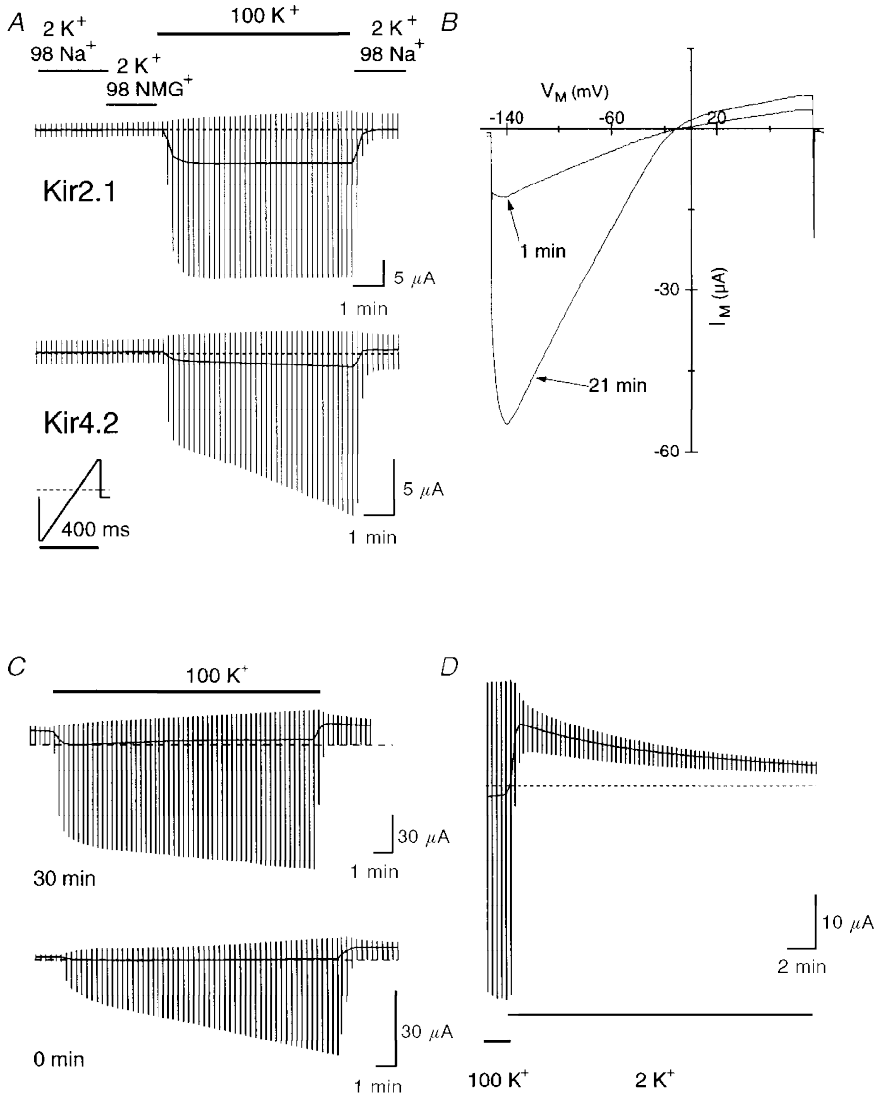

Figure 4. K^+ activation of mKir4.2 channels.

A, representative current records from oocytes expressing Kir1.1 or Kir4.2 channels show the time course of current activation in mKir4.2-injected oocytes. Inset shows the voltage-ramp protocol. Oocytes were clamped at −20 mV and ramped between −140 and 80 mV every 10 s. Slow time base record indicates current amplitudes measured at holding potential, −140 mV and 80 mV. Bath changes between solutions are indicated by bars (concentrations of ions given in mM). *B*, current records from an mLV1-expressing oocyte show increase in current amplitude from K^+ activation. Records are from a longer duration recording than that shown in *A*, and are shown on an expanded time scale. The oocyte was here ramped between −140 and 60 mV (timing the same as in *A*). Traces show current recorded at 1 min and 21 min after changing the bath from ND96 to KD98 solution. Current increased from −12·6 to 54·8 μA at −140 mV. No corrections were made for leak or Cl^- current. *C*, preincubation of oocytes in 100 mM K^+ increases the initial amplitude of the mKir4.2 current and slows the apparent rate of K^+ activation. Thirty minutes preincubation in KD98 solution increased the initial amplitude of current measured after ~2 min in ND96 solution. Subsequent change to KD98 solution shows that preincubated oocytes displayed less pronounced K^+ activation, although initial current amplitude was greater. Oocytes were clamped at −5 mV and ramped from −40 to 60 mV every 15 s. Bar indicates bath solution change to KD98 solution (~13 min) from ND96. Dashed line indicates zero current level. Concentrations of ions in mM. *D*, representative current trace showing slow recovery from K^+ activation. Cells were preincubated in KD98 for > 30 min before voltage clamping. Cells were held at −5 mV and ramped from − 40 to 60 mV every 20 s.

phenomenon thus appears to be distinct from the run-down phenomenon reported for Kir2.3 channels (Henry *et al.* 1996), where lowering $[Na^+]_o$ below ~50 mM (by substituting either K^+ or NMG^+) caused a slow inactivation of the channel. The voltage dependence of the whole-cell current does not change substantially during K^+ activation (Fig. 4*B* and 5*B*), showing that K^+ activation cannot be accounted for by the activation of an endogenous current with dissimilar voltage dependence or from a change in the degree of rectification of mKir4.2 (Fig. 5). Doi *et al.* (1996) studied a similar phenomenon that they had observed with Kir1.1 (called 'K^+ regulation') in which Kir1.1 activity was increased in high $[K^+]$ and decreased in low $[K^+]$ solutions. They found that the rate of K^+ activation was independent of intracellular pH (pH_i), but the rate of deactivation on changing to low K^+ solution was sensitive to changes in pH_i. While mKir4.2 channel activity is sensitive to changes in pH_i (see below), pH_i changes cannot account for K^+ activation, since K^+ activation persisted during channel inhibition caused by intracellular acidification (Fig. 6, compare pre-HCO_3^- with post-HCO_3^-). The endogenous Cl^- current often observed in oocytes also appears to be activated by exposure to high $[K^+]$ solutions (increasing outward current in Kir2.1-expressing cell, Fig. 4*A*), but while activated by high $[K^+]$ solutions, this

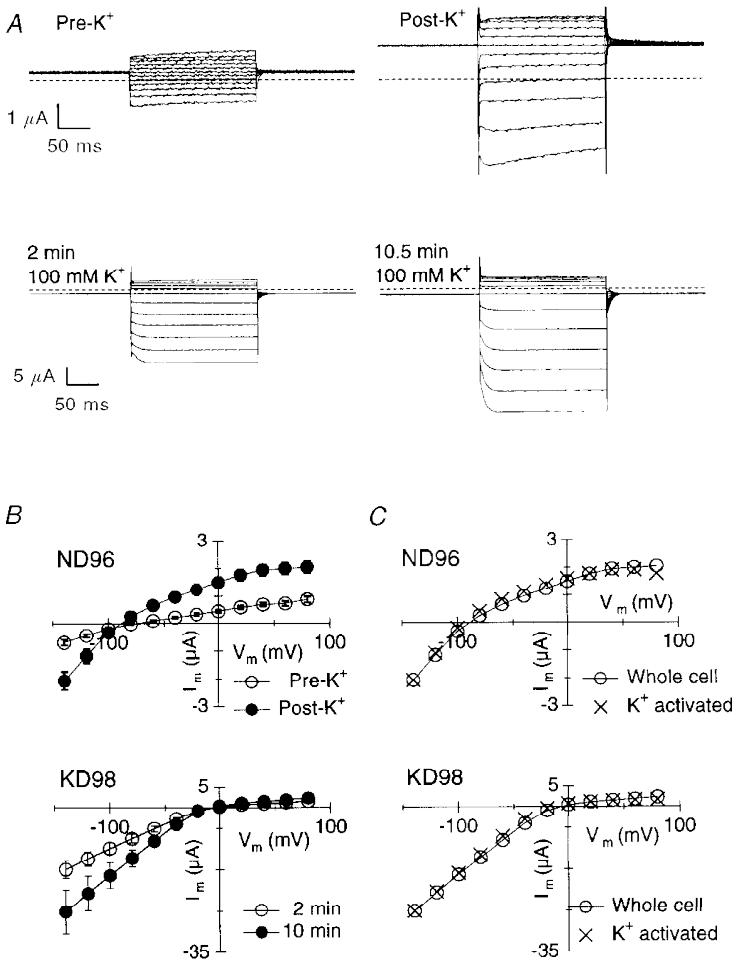

Figure 5. Voltage dependence of current activated during K^+ activation

A, current records from a representative oocyte during extended exposure to 100 mM K^+. Oocytes were clamped at −20 mV and stepped between −140 and 80 mV in 20 mV increments at 1 s intervals. Upper panel, current records in ND96 solution 2 min before (left) and 3 min after (right) a 12 min exposure to KD98 solution. Lower panel, current records in KD98 solution 2 min (left) and 10·5 min (right) after changing bath perfusion. *B*, averaged current–voltage relationships from 4 oocytes (exposed to K^+ as in *A*) measured at the end of each voltage step. Values represent whole-cell currents with no leak subtraction. Pre-K^+ currents were measured ~4 min prior to KD98 solution, and post-K^+ currents were measured 5 min after returning to ND96 solution. Error bars indicate S.E.M. *C*, difference currents (⊗) constructed by subtracting the initial currents shown in *B* from the later currents (i.e. in ND96, K^+ activated = Post-K^+ − Pre-K^+; in KD98, K^+ activated = 10 min − 2 min) and scaled to the amplitude of the whole-cell current at −140 mV (i.e. Post-K^+ for ND96; 10 min for KD98). Difference currents show the same intermediate rectification as whole-cell currents, indicating that the net current activated by high K^+ did not have a distinct voltage dependence compared with the Kir4.2 current.

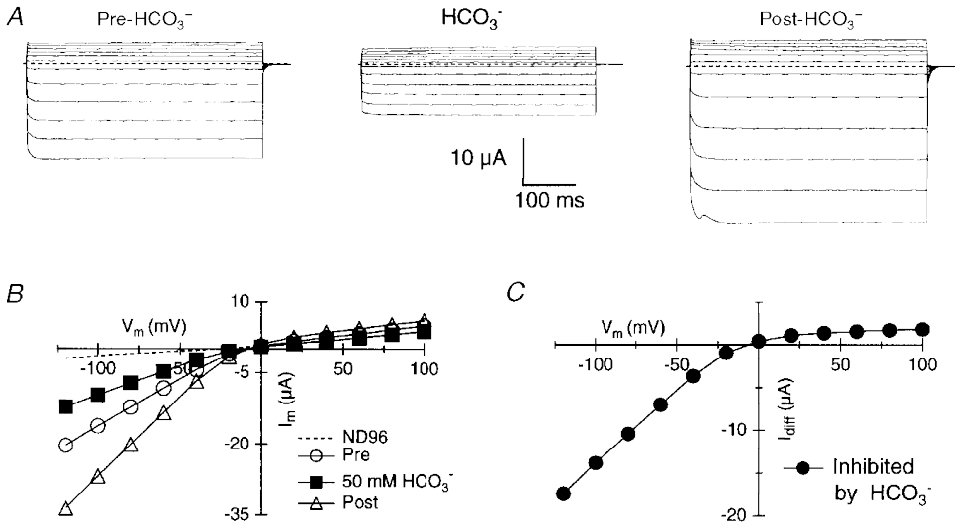

Figure 6. mKir4.2 current is reversibly inhibited by intracellular acidification

A, representative current traces recorded 1·5 min before, during (6 min from beginning), and 4 min after a 7·5 min application of 50 mM HCO_3^- to induce intracellular acidification. $[K^+]$ was held constant at 100 mM. Increase in current after HCO_3^- application results from the slow on-going activation of current seen in the presence of high $[K^+]_o$. *B*, current–voltage relationships measured at the end of test pulses from the currents shown in *A*. Dashed line shows current in 2 mM K^+. *C*, difference currents were constructed by subtracting current measured in 50 mM HCO_3^- from current measured before HCO_3^- plus estimated 'run-up' current from K^+ activation (see Methods).

current was also activated by low $[Na^+]$ solutions in which Na^+ had been replaced by NMG^+, and activation persisted for less time than activation of mKir4.2 (data not shown).

mKir4.2 current is reversibly inhibited by intracellular acidification. Kir1.1 channels (Tsai *et al.* 1995) and Kir4.1 channels (Shuck *et al.* 1997) have been shown to be very sensitive to small changes in intracellular pH. Acidification of the cytoplasm reversibly decreased Kir1.1 with a pK of ~6·8 (Tsai *et al.* 1995; Fakler *et al.* 1996). Intracellular acidification can be achieved by bathing oocytes in elevated $[HCO_3^-]_o$ solutions, causing CO_2 (aqueous) to diffuse into the cytoplasm and react with water to form H^+ and HCO_3^- (Fakler *et al.* 1996). Exposing mKir4.2-expressing oocytes to 50 mM HCO_3^- (replacing 50 mM Cl^-) caused a slow inhibition of current (64 ± 5%, $n = 6$). Current inhibition developed over ~5 min and recovered on returning to 0 mM HCO_3^- with a similar time course (Fig. 6). The slow time course of changes in current amplitude indicates that channel inhibition was not the result of channel block by HCO_3^- ions.

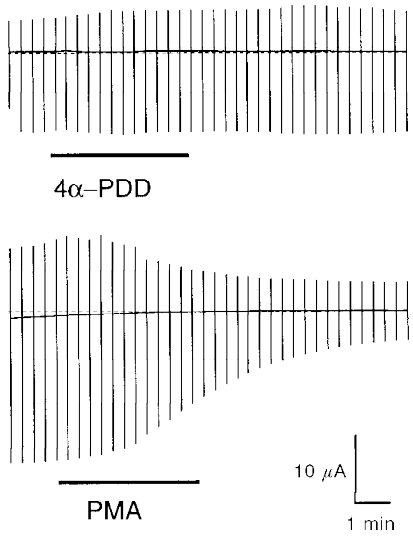

Figure 7. PKC activation inhibits mKir4.2

Time course records show currents measured from voltage ramps from −40 to 60 mV (holding potential, −5 mV). Approximately 4 min application of 200 nM 4α-PDD, an inactive phorbol ester, was without affect on membrane currents (upper trace), while application of 200 nM PMA, a phorbol ester activator of PKC, caused a pronounced slowly developing and persistent inhibition of mKir4.2 current (lower trace).

mLV1 current is inhibited by PKC activation. Consensus sites for phosphorylation by PKC exist at four loci (Fig. 1), indicating the potential for modulation by PKC. To examine the sensitivity of mKir4.2 to modulation by PKC, we activated endogenous PKC by applying phorbol esters (PMA or PDBU), which activate PKC. Phorbol ester application (100 nM–1 μM) caused a slow, persistent inhibition (64 $\pm$ 7 %, $n = 5$) of mKir4.2 current, while the inactive phorbol ester 4α-PDD did not affect the current ($n = 5$) (Fig. 7). The inhibition of mKir4.2 current by PKC activation was qualitatively similar to the inhibition of Kir2.3 reported previously (Henry *et al.* 1996).

Co-expression of mKir4.2 and Kir5.1 produces novel channel properties. Previous studies have shown that the rKir4.1 channel is capable of forming heteromultimeric channels with members of other subfamilies (Kir1.1, Kir2.1 and Kir5.1) (Glowatzki *et al.* 1995; Fakler *et al.* 1996; Pessia *et al.* 1996). Furthermore, attempts to co-express hKir4.2 with hKir4.1 or Kir1.1 caused a reduction in current compared with control cells injected with hKir4.1 or Kir1.1 alone (Shuck *et al.* 1997), suggesting that hKir4.2 can form heteromultimeric channels with hKir4.1 or Kir1.1. We thus hypothesized that, since hKir4.2 appears to form similar (though non-functional) heteromultimers as those formed by Kir4.1, mKir4.2 might form functional heteromultimers similar to those formed by Kir4.1. Because of the intermediate rectification of mKir4.2, heteromeric channels formed with either Kir1.1 or Kir2.1 may not be readily distinguishable from the rectification of either population of homomeric channels. Therefore, we chose to co-express mKir4.2 with rKir5.1, which does not form functional homomeric channels but which has been shown to form

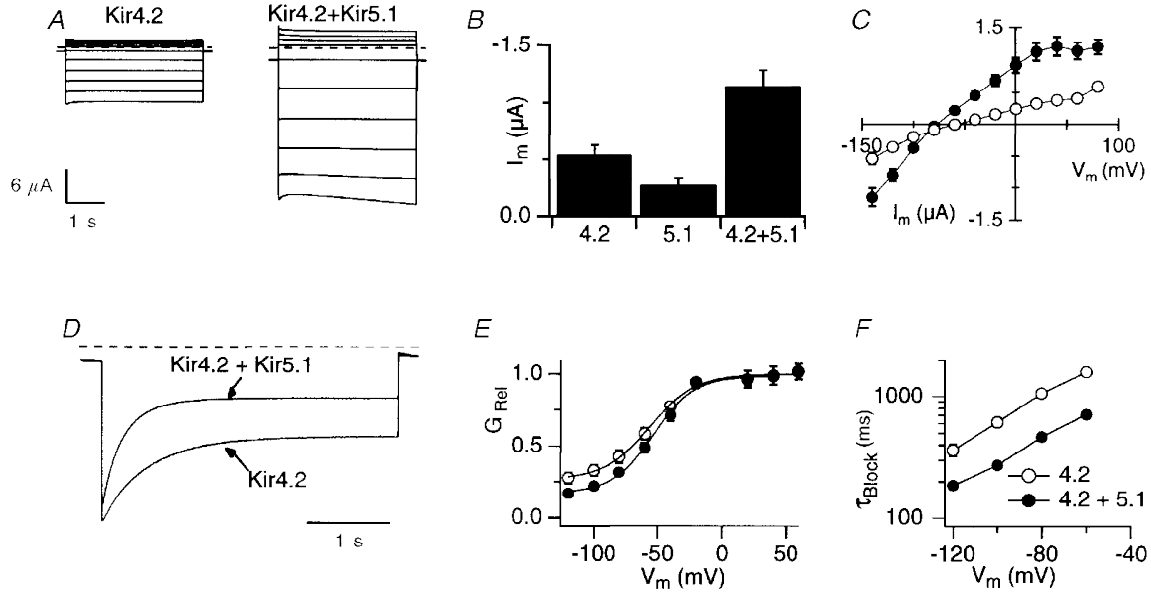

Figure 8. mKir4.2 forms heteromultimeric channels with Kir5.1

A, representative current traces of voltage-clamp records in KD98 solution from cells expressing mKir4.2 alone or co-expressing mKir4.2 and rKir5.1. Cells were held at −20 mV and stepped to potentials between −120 and 60 mV for 3·6 s every 5 s. The mKir4.2 currents are plotted at twice the gain of the currents from co-expressing cells. Note that at the most negative potentials, the cell co-expressing mKir4.2 and rKir5.1 exhibits pronounced inward current relaxations not present in cells expressing mKir4.2 alone. Co-expressing cells injected with a 4 : 1 ratio of Kir5.1 : Kir4.2 cRNA. *B*, comparison of initial current amplitude at −140 mV in ND96 solution. Oocytes injected with Kir5.1 had membrane currents similar to uninjected oocytes (data not shown) (means $\pm$ S.E.M.: Kir4.2, $n = 21$; Kir5.1, $n = 3$; Kir4.2 + Kir5.1, $n = 23$). No leak subtraction was employed. *C*, averaged current–voltage relationships for whole-cell current amplitude measured initially in ND96 solution. Cells were held at −20 mV and stepped between −140 and 80 mV for 200 ms every 1 s. Co-expressing cells injected with a 1 : 1 ratio of Kir5.1 : Kir4.2 cRNA. Same data set used as in *B*. *D*, representative current traces showing different kinetics of Ba^{2+} block in cells expressing mKir4.2 alone or co-expressing mKir4.2 and rKir5.1. Voltage protocol same as for *A*, with the step to −100 mV shown here, $[Ba^{2+}] = 10$ μM. Current traces have been plotted to the same amplitude at the holding potential to facilitate comparison of both the kinetics and the degree of block. Dashed line indicates zero current level. Co-expressing cells injected with a 4 : 1 ratio of Kir5.1 : Kir4.2 cRNA. *E*, conductance (G_{rel})–voltage relationships show that Ba^{2+} blocks current more effectively in co-expressing cells than in mono-expressing cells. Data plotted is for 10 μM Ba^{2+} (means $\pm$ S.E.M.; Kir4.2, $n = 4$; Kir4.2 + Kir5.1, $n = 3$). *F*, time constants measured for 10 μM Ba^{2+} block (means $\pm$ S.E.M.; same data set as in *E*). Block of current in co-expressing cells was twice as fast as in cells expressing mKir4.2 alone. A similar difference in blocking kinetics was apparent over this voltage range for $[Ba^{2+}]$ up to 500 μM.

functional heteromultimeric channels with distinct properties when co-expressed with rKir4.1 (Pessia *et al.* 1996). As previously reported, oocytes injected with cRNA for Kir5.1 alone displayed no discernible current compared with control oocytes (data not shown). However, oocytes co-injected with mKir4.2 and Kir5.1 cRNA displayed large currents. To quantify current amplitudes without the complication of K^+ activation, currents were measured in ND96 solution before exposure to high $[K^+]_o$. Oocytes co-expressing mKir4.2 and Kir5.1 had larger currents ($-1{\cdot}15 \pm 0{\cdot}14\ \mu$A at -140 mV, $n = 23$) than oocytes expressing mKir4.2 alone ($-0{\cdot}54 \pm 0{\cdot}09\ \mu$A at -140 mV, $n = 21$) (Fig. 8*B*), indicating that Kir5.1 either enhanced or altered the expression of mKir4.2, or that Kir5.1 formed heteromeric channels with mKir4.2 so that a larger net K^+ conductance was expressed in the oocytes due to an increase in number and/or unit conductance of single Kir channels. By using a fourfold reduction in the amount of mKir4.2 cRNA injected (for both co-expressing and mono-expressing oocytes) while injecting the same amount of Kir5.1 cRNA, no Kir current was apparent in ND96 solution for mKir4.2 oocytes, but was still apparent in co-injected oocytes (data not shown). On changing to KD98 solution, Kir currents were apparent in both sets of oocytes, but the current amplitude was much larger in co-injected cells and had distinct kinetic properties (Fig. 8*A*). For mKir4.2, long pulses to potentials below -80 mV produced inward currents that reached a plateau within ~200 ms, while for oocytes co-expressing mKir4.2 and Kir5.1 such pulses produced slow inward relaxations, similar to currents previously recorded in oocytes co-expressing Kir5.1 and rKir4.1 (Pessia *et al.* 1996). These novel gating kinetics strongly suggest that Kir5.1 is not simply increasing expression of mKir4.2, but rather that mKir4.2 and Kir5.1 are instead forming heteromultimeric channels with novel properties. To investigate further whether mKir4.2 and Kir5.1 formed heteromultimeric channels, we sought to determine if differences could be detected in the pore properties (such as channel block) of channels in co-expressing oocytes. Comparing mono-expressing and co-expressing oocytes with fourfold diluted mKir4.2 cRNA, no differences were found in Cs^+ block of the channel (data not shown) but Ba^{2+} was found to block the current more effectively in co-expressing oocytes (Fig. 8*C* and *D*). Using $[Ba^{2+}]$ from 5 μM to 1 mM, differences in steady-state block were most apparent at concentrations less than 100 μM and at potentials below -40 mV (Fig. 8*D*). The kinetics of current block by Ba^{2+} were also altered in co-expressing oocytes, with Ba^{2+} blocking inward current more rapidly than in oocytes expressing mKir4.2 alone (Fig. 8*C*). For most Ba^{2+} concentrations and membrane potentials, the time course of block could be fitted with a single exponential function for both mono-expressing and co-expressing oocytes. The time constants derived from these fits showed that Ba^{2+} block occurred twice as fast in oocytes co-expressing mKir4.2 and Kir5.1 as in oocytes expressing only mKir4.2 (Fig. 8*E*). Thus, currents from co-expressing oocytes had pore properties that were clearly distinguishable from those in oocytes expressing mKir4.2 alone, further indicating that mKir4.2 forms heteromultimeric channels with Kir5.1.

DISCUSSION

mLV1/mKir4.2 is a functional Kir4 channel. Kir channels now known to form functional heteromultimers (e.g. Kir3.1) have not generally been shown to pass current at high density when expressed as homomultimers in *Xenopus* oocytes. An ion channel with high sequence identity (96%) to the mKir4.2 channel has been cloned from human kidney and skeletal muscle by three other groups (Gosset *et al.* 1997; Ohira *et al.* 1997; Shuck *et al.* 1997), but the human clone was reported not to express functional channels in *Xenopus* oocytes, and to decrease the amplitude of current through Kir1.1 or Kir4.1 channels when oocytes were injected with a mixture of both RNAs (Shuck *et al.* 1997). In contrast, our data clearly show that *Xenopus* oocytes injected with mKir4.2 RNA express a large K^+ conductance that is not present in control oocytes. The current is K^+ selective and displays biophysical properties of inward rectifiers, including a conductance proportional to the square root of $[K^+]_o$, voltage-dependent block by extracellular Ba^{2+} and Cs^+, and low sensitivity to block by extracellular TEA. While other Kir4 family members (Bond *et al.* 1994; Bredt *et al.* 1995; Kubo *et al.* 1996; Shuck *et al.* 1997) can express homomultimeric channels in oocytes, Kir4.1 has additionally been shown to form novel functional heteromultimeric channels with Kir5.1 (Pessia *et al.* 1996), a channel protein which does not express functional homomeric channels, as well as with Kir2.1 (Fakler *et al.* 1996) and Kir1.1 (Glowatzki *et al.* 1995). Kir4.1 has also been shown to interact with PSD-95 family proteins (Horio *et al.* 1997). Co-expression of Kir4.1 and PSD-95 family proteins in HEK293 cells increased the amplitude of Kir4.1 current compared with the amplitude of Kir4.1 current in cells expressing Kir4.1 alone, suggesting that PSD-95 expression increased the efficiency of channel formation. PSD-95 family members are membrane associated proteins known to interact with several types of ion channel proteins and apparently induce clustering of the channels in the plasma membrane by interacting with the Ser/Thr–X–Val sequence at the C-terminus of the ion channel protein (Kim *et al.* 1995; Kornau *et al.* 1995). This motif is present at the C-terminus of all identified Kir4 channels. Together with our present results, the weight of evidence indicates that, while Kir4 proteins may interact and associate with several other classes of protein, they do not require another protein for expression of functional channels. Further studies will be needed to determine why the human clone of Kir4.2 did not express functional channels (Shuck *et al.* 1997) while the mouse clone did. It is possible that the lack of functional channel expression may be related to the K^+ activation effect. If the human clone is even more sensitive to K^+ activation than the mouse clone (or activated more slowly), the duration of the experiment may have been too short to detect current. On the other hand, structural differences

between the human and mouse clone may be significant enough to account for loss of function of the human clone. In particular, five varying residues located (presumably) on the extracellular mouth of the pore between the M1 and H5 regions are prime candidates for diminishing channel function, since mutations in homologous regions of Kir1.1 have been associated with antenatal Bartter's syndrome (International Collaborative Study Group for Bartter-like Syndromes, 1997), a renal disorder that can result from loss of function of the Kir1.1 channel.

Classification of Kir families. The classification of channels closely related to the channel we termed 'mLV1' is at present confused. The human clone has been classified as either Kir1.3 (Shuck *et al.* 1997) or Kir4.2 (Gosset *et al.* 1997), and a third report did not attempt to place the channel into the numeric nomenclature (Ohira *et al.* 1997). The classification of this channel as Kir1.3 was based on its homology with a channel cloned at the same time designated and Kir1.2 (Shuck *et al.* 1997), which was in fact the human homologue of a channel previously cloned from rat and originally classified as Kir4.1 (Bond *et al.* 1994; Doupnik *et al.* 1995). The report classifying the human mLV1 homologue as Kir4.2 (Gosset *et al.* 1997) based the classification on homology to the rat Kir4.1 channel (Bond *et al.* 1994; Takumi *et al.* 1995). However, the cloning of a novel channel from salmon brain, sWIRK (Kubo *et al.* 1996), was published before any of the reports of the human clone. As sWIRK is more closely related to the mLV1 clones and the Kir4.1 channel than to Kir1.1, it seems logical to retain both Kir1 and Kir4 subfamilies, and to include both mLV1 and sWIRK in the Kir4 subfamily. While the cloning of sWIRK was reported prior to the cloning of mLV1 or its human homologue and should thus perhaps be designated Kir4.2, this designation has already been used in a published report for the human clone (Gosset *et al.* 1997). We thus suggest that mLV1 should be regarded as mKir4.2 to prevent further confusion, and that sWIRK be regarded as sKir4.3.

Comparison to other Kir channels. The cloning and subsequent mutation of many Kir channels has identified several regions and specific amino acid residues that are associated with specific biophysical properties of the channels. mKir4.2 channels displayed many properties predicted by the presence of several motifs in the amino acid sequence, including intracellular pH sensitivity and PKC-induced inhibition. Both Kir1.1 and Kir4.1 channels have been shown to be inhibited by intracellular acidification (Tsai *et al.* 1995; Shuck *et al.* 1997), and both contain the lysine residue (mKir4.2 Lys66) immediately before the M1 transmembrane domain, which has been implicated in conferring pH sensitivity on Kir1.1 channels (Fakler *et al.* 1996). The presence of a glutamic acid residue at position 157 predicts that the channel will display strong rectification due to channel block by Mg^{2+} and polyamines (Fakler *et al.* 1994; Ficker *et al.* 1994; Lopatin *et al.* 1994; Lu & MacKinnon, 1994). While mKir4.2 channels rectify more strongly than Kir1.1 channels, the rectification is weaker than seen for many Kir channels with aspartic acid residues in the corresponding 'rectification controller' position (i.e. Kir2.1, Kir2.3, Kir1.1 N171D). Intermediate rectification has also been reported for Kir4.3 (Kubo *et al.* 1996), and Kir4.1 (Bond *et al.* 1994; Takumi *et al.* 1995; Shuck *et al.* 1997), both of which also possess glutamic acid residues at the 'rectification controller' position, although rectification is identical in Kir6.2 N160D and N160E channels (Shyng *et al.* 1997). mKir4.2 lacks a second acidic residue that is present in the C-terminal cytoplasmic tail and contributes to the strong rectification of Kir2 channels (Yang *et al.* 1995). This may underlie the weaker rectification of mKir4.2 compared with Kir2 channels.

Co-expression studies found that mKir4.2 interacts with Kir5.1 to produce currents with properties distinct from mKir4.2 current or the non-functional Kir5.1 channel, indicating that mKir4.2 and Kir5.1 probably form heteromeric channels. This is consistent with the finding that Kir4.1 and Kir5.1 interact to form heteromeric channels (Pessia *et al.* 1996), and shows further that Kir4.1 and Kir4.2 have not only structural but also functional similarities. While several other channels have been shown to form heteromeric channels with Kir4.1, no other channel has thus far been shown to form functional channels with Kir5.1. The mechanism by which Kir4.1 and now Kir4.2 rescue the function of Kir5.1 is unknown.

Modulation of mKir4.2. While mKir4.2 current does not display strong voltage dependence, it is susceptible to modulation by several apparently distinct mechanisms. In addition to sensitivity to intracellular pH and PKC activity, mKir4.2 channels are also sensitive to $[K^+]_o$, the currents slowly increasing on continued exposure to elevated $[K^+]_o$. The slow time course of K^+ activation suggests that the phenomenon may be a secondary consequence of a cellular process rather than from a direct effect of K^+ on the channel, since solution changes were complete in a relatively short time (1 min for solution change compared with current increases continuing for 60 min). An apparently similar process, termed K^+ regulation, has also been reported for Kir1.1 channels (Doi *et al.* 1996). In Kir1.1, K^+ regulation was found to be modulated, but not mediated, by intracellular pH. Doi *et al.* (1996) found that exposure to high concentrations of K^+, Cs^+ or Rb^+ increased Kir1.1 activity, while high concentrations of Na^+ or Li^+ decreased Kir1.1 activity. Furthermore, the rate of reversal of activation on switching from a high $[K^+]_o$ to low $[K^+]_o$ solution was increased with intracellular acidification. Studies with Kir2.1–Kir1.1 channel chimeras showed that the 'core region' (i.e. M1–H5–M2 domains) of Kir1.1 channels conferred K^+ regulation, but that pH sensitivity of K^+ regulation was conferred by the N-terminus, which also confers pH sensitivity on Kir1.1 channels (Fakler *et al.* 1996). Because K^+ regulation of Kir1.1 was studied with different experimental protocols than we used to study K^+ activation of mKir4.2, it is difficult to compare the properties of the

two processes directly. However, K^+ regulation of Kir1.1 was shown to activate over 10 min, while K^+ activation of mKir4.2 continued for a longer time (as long as 1 h), suggesting that differences exist in the K^+ sensitivity of these two channels, although a quantitative comparison of K^+ sensitivity in Kir1.1 and Kir4.2 channels would require direct comparison of the process with channels expressed in oocytes from the same batch. Preliminary studies (not shown) indicate that activation of mKir4.2 can also be produced by high concentrations of Cs^+ and Rb^+, but not Li^+ or Na^+, as seen for Kir1.1. While the significance of K^+ activation is at this point unclear, further study of the phenomenon may reveal an as yet unknown mechanism of channel modulation. The combined sensitivity to intracellular pH, PKC activity, and extracellular $[K^+]$ may be unique to the mKir4.2 channel (among the channels known to be sensitive to intracellular pH); there are, as yet, no reports about PKC- or K^+-dependent modulation for Kir4.1 or sKir4.3, and Kir1.1 has been shown to be insensitive to activation of PKC (Henry *et al.* 1996).

All Kir4 subfamily clones reported so far have shown a relatively restricted distribution in animal tissues. Kir4.1 RNA has been localized primarily in kidney and glial cells of the brain (Bredt *et al.* 1995; Takumi *et al.* 1995; Ito *et al.* 1996; Kubo *et al.* 1996) as well as in marginal cells of the stria vascularis in the cochlea (Hibino *et al.* 1997), while human Kir4.2 RNA has been localized in kidney, lung, and pancreas (Ohira *et al.* 1997; Shuck *et al.* 1997). A third group additionally reports cloning two isoforms of the gene (with differing 5′ untranslated sequences) from adult skeletal muscle and fetal brain, with Northern blot analysis showing localization primarily in the kidney, but also in pancreas, lung, leukocytes, heart, and brain (Gosset *et al.* 1997). Interestingly, genomic localization of Kir4.2 shows that it is one of several genes located on a 2·5 megabase region of chromosome 21 essential for conferring the main phenotypic characteristics of Down's syndrome (trisomy 21) (Gosset *et al.* 1997; Ohira *et al.* 1997). As we cloned this channel from liver tissue, it is somewhat surprising that reports of cloning the human homologue of this gene found no evidence of its presence in human liver with Northern blot analysis (Gosset *et al.* 1997; Ohira *et al.* 1997; Shuck *et al.* 1997). This may indicate that the Kir4.2 channel is present at a low level in a wider tissue distribution than shown previously. The membrane potential of rat hepatocytes is sensitive to changes in intracellular pH, and acidification of the cytoplasm depolarizes the cell (Bear *et al.* 1988). As this depolarization can be abolished by the K^+ channel blockers Ba^{2+} and quinine, or by elevating extracellular $[K^+]$, it was concluded that the depolarization was mediated by the pH-dependent closure of K^+ channels. Although the physiological relevance of this phenomenon is unknown, the pH-sensitive Kir4.2 channel is a good candidate for mediating this phenomenon. Kir4.2 channels may also participate in modulating plasma $[K^+]$ observed during intravascular infusion of adrenergic agonists in mammals, as the liver has been implicated as the site of K^+ uptake during the hypokalaemia that is induced during prolonged infusion of dopamine or dobutamine (Drake *et al.* 1989). A more likely physiological role for Kir4.2 is in renal function, since other investigators have shown high levels of Kir4.2 RNA expression in the kidney (Shuck *et al.* 1997). Recent reports have shown that an inward rectifier K^+ channel is expressed on the basolateral membrane of cells from the proximal tubule of the amphibian kidney (Mauerer *et al.* 1998*a*), and that these channels are subject to modulation by PKC and intracellular pH in a similar manner to that found with Kir4.2 (Mauerer *et al.* 1998*b*). The proximal tubule is responsible for the majority of Na^+, K^+, Cl^- and H_2O reabsorption in the kidney, which is driven by the Na^+ gradient across the apical membrane that is created by the activity of Na^+,K^+-ATPase in the basolateral membrane. The energy of the Na^+ gradient is used to drive reabsorption of a variety of solutes from the lumen of the tubule through Na^+-coupled cotransporters in the apical membrane. The high activity of the basolateral membrane Na^+,K^+-ATPase required to maintain this gradient produces a large basolateral K^+ influx. Additional (Na^+-coupled) K^+ influx from the apical surface in combination with the basolateral K^+ influx requires an exit pathway for K^+ at the basolateral membrane to maintain K^+ homeostasis. K^+ channels such as the Kir4.2 channel or those characterized by Mauerer *et al.* (1988*a*,*b*), which conduct current over a wide range of membrane potentials and which are subject to modulation by a variety of effectors, provide a basolateral K^+ conductance well suited to the task of maintaining K^+ homeostasis in the cells of the proximal tubule under highly variable tubular solute concentrations.

Appel, R. D., Bairoch, A. & Hochstrasser, D. F. (1994). A new generation of information retrieval tools for biologists: the example of the ExPASy WWW server. *Trends in Biochemical Sciences* **19**, 258–260.

Bear, C. E., Davison, J. S. & Shaffer, E. A. (1988). Intracellular pH influences the resting membrane potential of isolated rat hepatocytes. *Biochimica et Biophysica Acta* **944**, 113–120.

Bond, C. T., Pessia, M., Xia, X. M., Lagrutta, A., Kavanaugh, M. P. & Adelman, J. P. (1994). Cloning and expression of a family of inward rectifier potassium channels. *Receptors and Channels* **2**, 183–191.

Bredt, D. S., Wang, T. L., Cohen, N. A., Guggino, W. B. & Snyder, S. H. (1995). Cloning and expression of two brain-specific inwardly rectifying potassium channels. *Proceedings of the National Academy of Sciences of the USA* **92**, 6753–6757.

Chuang, H., Jan, Y. N. & Jan, L. Y. (1997). Regulation of IRK3 inward rectifier K^+ channel by m1 acetylcholine receptor and intracellular magnesium. *Cell* **89**, 1121–1132.

Cohen, N. A., Sha, Q., Makhina, E. N., Lopatin, A. N., Linder, M. E., Snyder, S. H. & Nichols, C. G. (1996). Inhibition of an inward rectifier potassium channel (Kir2·3) by G-protein $\beta\gamma$ subunits. *Journal of Biological Chemistry* **271**, 32301–32305.

Collins, A., German, M. S., Jan, Y. N., Jan, L. Y. & Zhao, B. (1996). A strongly inwardly rectifying K^+ channel that is sensitive to ATP. *Journal of Neuroscience* **16**, 1–9.

Coulter, K. L., Perier, F., Radeke, C. M. & Vandenberg, C. A. (1995). Identification and molecular localization of a pH-sensing domain for the inward rectifier potassium channel HIR. *Neuron* **15**, 1157–1168.

Doi, T., Fakler, B., Schultz, J. H., Schulte, U., Brandle, U., Weidemann, S., Zenner, H. P., Lang, F. & Ruppersberg, J. P. (1996). Extracellular K^+ and intracellular pH allosterically regulate renal Kir1.1 channels. *Journal of Biological Chemistry* **271**, 17261–17266.

Doupnik, C. A., Davidson, N. & Lester, H. A. (1995). The inward rectifier potassium channel family. *Current Opinion in Neurobiology* **5**, 268–277.

Drake, H. F., Smith, M., Corfield, D. R. & Treasure, T. (1989). Continuous multi-channel intravascular monitoring of the effects of dopamine and dobutamine on plasma potassium in dogs. *Intensive Care Medicine* **15**, 446–451.

Fakler, B., Brandle, U., Bond, C., Glowatzki, E., Konig, C., Adelman, J. P., Zenner, H. P. & Ruppersberg, J. P. (1994). A structural determinant of differential sensitivity of cloned inward rectifier K^+ channels to intracellular spermine. *FEBS Letters* **356**, 199–203.

Fakler, B., Schultz, J. H., Yang, J., Schulte, U., Brandle, U., Zenner, H. P., Jan, L. Y. & Ruppersberg, J. P. (1996). Identification of a titratable lysine residue that determines sensitivity of kidney potassium channels (ROMK) to intracellular pH. *EMBO Journal* **15**, 4093–4099.

Ficker, E., Taglialatela, M., Wible, B. A., Henley, C. M. & Brown, A. M. (1994). Spermine and spermidine as gating molecules for inward rectifier K^+ channels. *Science* **266**, 1068–1072.

Glowatzki, E., Fakler, G., Brandle, U., Rexhausen, U., Zenner, H. P., Ruppersberg, J. P. & Fakler, B. (1995). Subunit-dependent assembly of inward-rectifier K^+ channels. *Proceedings of the Royal Society of London* B **261**, 251–261.

Gosset, P., Ghezala, G. A., Korn, B., Yaspo, M. L., Poutska, A., Lehrach, H., Sinet, P. M. & Creau, N. (1997). A new inward rectifier potassium channel gene (KCNJ15) localized on chromosome 21 in the Down syndrome chromosome region 1 (DCR1). *Genomics* **44**, 237–241.

Hagiwara, S. & Takahashi, K. (1974). The anomalous rectification and cation selectivity of the membrane of a starfish egg cell. *Journal of Membrane Biology* **18**, 61–80.

Henry, P., Pearson, W. L. & Nichols, C. G. (1996). Protein kinase C inhibition of cloned inward rectifier (HRK1/KIR2·3) K^+ channels expressed in *Xenopus* oocytes. *Journal of Physiology* **495**, 681–688.

Hibino, H., Horio, Y., Inanobe, A., Doi, K., Ito, M., Yamada, M., Gotow, T., Uchiyama, Y., Kawamura, M., Kubo, T. & Kurachi, Y. (1997). An ATP-dependent inwardly rectifying potassium channel, KAB-2 (Kir4.1), in cochlear stria vascularis of inner ear: its specific subcellular localization and correlation with the formation of endocochlear potential. *Journal of Neuroscience* **17**, 4711–4721.

Ho, K., Nichols, C. G., Lederer, W. J., Lytton, J., Vassilev, P. M., Kanazirska, M. V. & Hebert, S. C. (1993). Cloning and expression of an inwardly rectifying ATP-regulated potassium channel. *Nature* **362**, 31–38.

Horio, Y., Hibino, H., Inanobe, A., Yamada, M., Ishii, M., Tada, Y., Satoh, E., Hata, Y., Takai, Y. & Kurachi, Y. (1997). Clustering and enhanced activity of an inwardly rectifying potassium channel, Kir4.1, by an anchoring protein, PSD-95/SAP90. *Journal of Biological Chemistry* **272**, 12885–12888.

Inagaki, N., Gonoi, T., Clement, J. P., Namba, N., Inazawa, J., Gonzalez, G., Aguilar-Bryan, L., Seino, S. & Bryan, J. (1995). Reconstitution of I_{KATP}: an inward rectifier subunit plus the sulfonylurea receptor. *Science* **270**, 1166–1170.

International Collaborative Study Group for Bartter-like Syndromes, (1997). Mutations in the gene encoding the inwardly-rectifying renal potassium channel, ROMK, cause the antenatal variant of Bartter syndrome: evidence for genetic heterogeneity. *Human Molecular Genetics* **6**, 17–26.

Ito, M., Inanobe, A., Horio, Y., Hibino, H., Isomoto, S., Ito, H., Mori, K., Tonosaki, A., Tomoike, H. & Kurachi, Y. (1996). Immunolocalization of an inwardly rectifying K^+ channel, KAB-2 (Kir4.1), in the basolateral membrane of renal distal tubular epithelia. *FEBS Letters* **388**, 11–15.

Kim, E., Niethammer, M., Rothschild, A., Jan, Y. N. & Sheng, M. (1995). Clustering of *Shaker*-type K^+ channels by interaction with a family of membrane-associated guanylate kinases. *Nature* **378**, 85–88.

Kornau, H. C., Schenker, L. T., Kennedy, M. B. & Seeburg, P. H. (1995). Domain interaction between NMDA receptor subunits and the postsynaptic density protein PSD-95. *Science* **269**, 1737–1740.

Kozak, M. (1987). At least six nucleotides preceding the AUG initiator codon enhance translation in mammalian cells. *Journal of Molecular Biology* **196**, 947–950.

Krapivinsky, G., Gordon, E. A., Wickman, K., Velimirovic, B., Krapivinsky, L. & Clapham, D. E. (1995). The G-protein-gated atrial K^+ channel I_{KACh} is a heteromultimer of two inwardly rectifying K^+-channel proteins. *Nature* **374**, 135–141.

Kubo, Y., Baldwin, T. J., Jan, Y. N. & Jan, L. Y. (1993). Primary structure and functional expression of a mouse inward rectifier potassium channel. *Nature* **362**, 127–133.

Kubo, Y., Miyashita, T. & Kubokawa, K. (1996). A weakly inward rectifying potassium channel of the salmon brain. Glutamate 179 in the second transmembrane domain is insufficient for strong rectification. *Journal of Biological Chemistry* **271**, 15729–15735.

Lopatin, A. N., Makhina, E. N. & Nichols, C. G. (1994). Potassium channel block by cytoplasmic polyamines as the mechanism of intrinsic rectification. *Nature* **372**, 366–369.

Lu, Z. & MacKinnon, R. (1994). Electrostatic tuning of Mg^{2+} affinity in an inward-rectifier K^+ channel. *Nature* **371**, 243–246.

Mauerer, U. R., Boulpaep, E. L. & Segal, A. S. (1998*a*). Properties of an inwardly rectifying ATP-sensitive K^+ channel in the basolateral membrane of renal proximal tubule. *Journal of General Physiology* **111**, 139–160.

Mauerer, U. R., Boulpaep, E. L. & Segal, A. S. (1998*b*). Regulation of an inwardly rectifying ATP-sensitive K^+ channel in the basolateral membrane of renal proximal tubule. *Journal of General Physiology* **111**, 161–180.

Nichols, C. G. & Lopatin, A. N. (1997). Inward rectifier potassium channels. *Annual Review of Physiology* **59**, 171–191.

Ohira, M., Seki, N., Nagase, T., Suzuki, E., Nomura, N., Ohara, O., Hattori, M., Sakaki, Y., Eki, T., Murakami, Y., Saito, T., Ichikawa, H. & Ohki, M. (1997). Gene identification in 1·6-Mb region of the Down syndrome region on chromosome 21. *Genome Research* **7**, 47–58.

Pessia, M., Tucker, S. J., Lee, K., Bond, C. T. & Adelman, J. P. (1996). Subunit positional effects revealed by novel heteromeric inwardly rectifying K^+ channels. *EMBO Journal* **15**, 2980–2987.

Reuveny, E., Slesinger, P. A., Inglese, J., Morales, J. M., Iniguez-Lluhi, J. A., Lefkowitz, R. J., Bourne, H. R., Jan, Y.N. & Jan, L. Y. (1994). Activation of the cloned muscarinic potassium channel by G protein $\beta\gamma$ subunits. *Nature* **370**, 143–146.

Shuck, M. E., Piser, T. M., Bock, J. H., Slightom, J. L., Lee, K. S. & Bienkowski, M. J. (1997). Cloning and characterization of two K^+ inward rectifier (Kir) 1.1 potassium channel homologs from human kidney (Kir1.2 and Kir1.3). *Journal of Biological Chemistry* **272**, 586–593.

Shyng, S., Ferrigni, T. & Nichols, C. G. (1997). Control of rectification and gating of cloned KATP channels by the Kir6.2 subunit. *Journal of General Physiology* **110**, 141–153.

Takumi, T., Ishii, T., Horio, Y., Morishige, K., Takahashi, N., Yamada, M., Yamashita, T., Kiyama, H., Sohmiya, K., Nakanishi, S. & Kurachi, Y. (1995). A novel ATP-dependent inward rectifier potassium channel expressed predominantly in glial cells. *Journal of Biological Chemistry* **270**, 16339–16346.

Tsai, T. D., Shuck, M. E., Thompson, D. P., Bienkowski, M. J. & Lee, K. S. (1995). Intracellular H^+ inhibits a cloned rat kidney outer medulla K^+ channel expressed in *Xenopus* oocytes. *American Journal of Physiology* **268**, C1173–1178.

Wei, A., Solaro, C., Lingle, C. & Salkoff, L. (1994). Calcium sensitivity of BK-type K_{Ca} channels determined by a separable domain. *Neuron* **13**, 671–681.

Yang, J., Jan, Y. N. & Jan, L. Y. (1995). Control of rectification and permeation by residues in two distinct domains in an inward rectifier K^+ channel. *Neuron* **14**, 1047–1054.

Acknowledgements

We are grateful for the assistance of Alice Butler in sequencing the mLV1 clone. We would also like to thank Dr N. Gautam (Departments of Anesthesiology and Genetics, Washington University School of Medicine) for providing the mouse liver cDNA library, Drs D. Hanck and L. Philipson (University of Chicago) for providing the Kir2.1 clone, and Dr J. Adelman (Oregon Health Sciences University) for providing the Kir5.1 clone. This work was supported by grant HL54171 to C.G.N., grants from the NIH to L.S., and a fellowship from the Washington University Cardiovascular Pharmacology Training Grant to W.L.P.

Corresponding author

W. L. Pearson: Renal Division, Washington University School of Medicine, Box 8126, 660 South Euclid Avenue, St Louis, MO 63110, USA.

Email: wpearson@cellbio.wustl.edu

Author's present address

M. Dourado: University of California, San Francisco, Department of Stomatology, 513 Parnassus Street, San Francisco, CA 94143-0512, USA.